



Universiteit
Leiden
The Netherlands

The role of inflammation in cardiac and vascular remodelling

Jong, R.C.M. de

Citation

Jong, R. C. M. de. (2019, January 31). *The role of inflammation in cardiac and vascular remodelling*. Retrieved from <https://hdl.handle.net/1887/68468>

Version: Not Applicable (or Unknown)

License: [Licence agreement concerning inclusion of doctoral thesis in the Institutional Repository of the University of Leiden](#)

Downloaded from: <https://hdl.handle.net/1887/68468>

Note: To cite this publication please use the final published version (if applicable).

Cover Page



Universiteit Leiden



The handle <http://hdl.handle.net/1887/68468> holds various files of this Leiden University dissertation.

Author: Jong, R.C.M. de

Title: The role of inflammation in cardiac and vascular remodelling

Issue Date: 2019-01-31

Chapter 3

Anti phosphorylcholine antibodies preserve cardiac function and reduce infarct size by attenuation of the inflammatory response following myocardial ischemia-reperfusion injury

Submitted for publication

Niek J. Pluijmert^{1*}

Rob C. M. de Jong^{2,3*}

Margreet R. de Vries^{2,3}

Knut Pettersson⁴

Douwe E. Atsma¹

J. Wouter Jukema^{1,3}

Paul H. A. Quax^{2,3}

* Authors contributed equally to this work

¹Department of Cardiology Leiden University Medical Center, Leiden, the Netherlands

²Department of Surgery, Leiden University Medical Center, Leiden, the Netherlands

³Einthoven Laboratory for Experimental Vascular Medicine,
Leiden University Medical Center, Leiden, the Netherlands

⁴Athera Biotechnologies, Stockholm, Sweden

Abstract

Background: Myocardial infarction is preceded by atherosclerosis and followed by a post-ischemic inflammatory process. Antibodies against phosphorylcholine (PC) are known to have anti-inflammatory properties.

Objectives: This study aimed to investigate the modulatory effects of a fully humanized IgG monoclonal antibody directed against phosphorylcholine (PC-mAb) in myocardial remodeling and cardiac function following myocardial ischemia-reperfusion (MI-R) injury.

Methods: In hypercholesterolemic ApoE*3-Leiden mice the LAD coronary artery was occluded for 45 minutes followed by permanent reperfusion and treatment with PC-mAb or vehicle. Two days and three weeks post reperfusion left ventricular (LV) function and infarct size (IS) were assessed by cardiac magnetic resonance imaging. LV fibrous content, LV wall thickness and leukocyte infiltration were evaluated (immuno) histologically. The systemic inflammatory response was analyzed using ELISA and FACS.

Results: Contrast-enhanced MRI assessed IS as well as histologically assessed LV fibrous content were reduced following PC-mAb treatment compared to vehicle three weeks post reperfusion. This resulted in reduced end-diastolic and end-systolic volumes by 24% and 42% respectively, leading to an increased ejection fraction by 33% in the PC-mAb group. These observations could be explained by a reduced systemic inflammatory response two days after reperfusion as observed by decreased CCL2 levels and circulating Ly6C^{hi} monocytes, resulting in reduced leukocyte infiltration and preservation of LV wall thickness after three weeks.

Conclusions: PC-mAb treatment attenuates the post-ischemic inflammatory response, leading to a reduction in adverse cardiac remodeling and preservation of cardiac function in hypercholesterolemic ApoE*3-Leiden mice. Therefore, PC-mAb therapy may be a valid therapeutic approach against MI-R injury.

Introduction

Ischemic heart disease remains one of the leading causes of death worldwide¹. Currently, the preferred therapy to treat acute myocardial infarction is revascularization therapy to salvage myocardium². However, revascularization causes a subsequent problem of myocardial ischemia-reperfusion (MI-R) injury, in which an additional wave of damage is inflicted to the myocardium due to an increased inflammatory response³ and generation of reactive oxygen species (ROS)⁴, ultimately leading to increased cell death. In a clinical perspective, MI-R injury contributes to adverse cardiac remodeling which subsequently leads to chronic heart failure, known as an important contributor of morbidity and mortality worldwide³. Currently, ameliorating this post-ischemic inflammatory process and healing of ischemic myocardium to inhibit LV remodelling remains a challenge.

The increased inflammatory response during MI-R injury is partially responsible for the increased generation of ROS⁴. These ROS are, at their turn, responsible for the formation of oxidation-damaged molecules, which can be recognized by the innate immune system⁵. Oxidation-damaged molecules are recognized by the innate immune system via so-called oxidation specific epitopes (OSEs), which can act as damage associated molecular patterns (DAMPs)⁵ and trigger toll-like receptors which play an important role in post MI remodeling^{6,7}. In this way inflammation and ROS generation increase each other's adverse effects following MI-R injury.

Following MI-R injury apoptotic cells express OSE on their outer membrane in the form of oxidized membrane phospholipids⁸. Phosphorylcholine (PC) is the polar head group of the membrane phospholipid phosphatidylcholine and an example of such an OSE, which is expressed on apoptotic cells, but interestingly not on viable cells⁸. Furthermore, apoptotic cells expressing PC, or other OSEs, are known for their immunogenic and pro-inflammatory properties⁸. Interestingly, PC is also expressed by oxidized LDL (oxLDL), an important lipoprotein in the development of atherosclerosis due to its pro-inflammatory properties⁵. Plasma levels of oxPL are in turn related to an increased risk of coronary artery disease events⁹. These PC containing proteins are targeted by innate immunity through recognition by scavenger receptors and natural antibodies¹⁰.

Natural antibodies against PC, also known as EO6 or T15 antibodies¹¹, are capable to inhibit oxLDL and apoptotic cell uptake by macrophages *in vitro*^{12,13}. Furthermore, it has been shown that EO6/T15 antibodies block the pro-inflammatory effects of PC expressing oxidation-damaged molecules^{8,14}. In addition, it has been shown that B-1a and B-1b cells produce atheroprotective OSE specific antibodies¹⁵⁻¹⁷, and sterile inflammation in the spleen initiates OSE specific antibody production by splenic B-cells which reduce the development of atherosclerosis¹⁸. Low concentrations of natural IgM anti-PC antibodies are associated with increased risk for cardiovascular diseases¹⁹⁻²² and acute coronary syndrome patients with low anti-PC antibody levels experience a

worsened prognosis²³. Active and passive immunization with antibodies against PC reduces atherosclerosis development^{24,25} and vein graft plaque size²⁶. Altogether, these data indicate that blocking PC using IgM antibodies may be an interesting approach to treat cardiovascular disease. However, IgM antibodies are not optimal for therapeutic use, because they are, compared to IgG antibodies, relatively expensive and difficult to produce.

Previously we developed PC-mAb, a fully humanized IgG against human PC with anti-inflammatory properties which reduces accelerated atherosclerosis development²⁷. In this study we used PC-mAb to investigate its effect against MI-R injury. This study was performed in a model trying to simulate the clinical setting of patients suffering from MI-R injury as a result of revascularization therapy. Therefore we used hypercholesterolemic ApoE*3-Leiden mice starting treatment after reperfusion and using a follow-up of three weeks.

Methods

Myocardial ischemia-reperfusion (MI-R) injury was induced in 12-14 weeks old female ApoE*3-Leiden mice as described previously²⁸. Subsequently mice were treated with 10 mg/kg PC-mAb every 3rd day or NaCl 0.9% w/v as a control (vehicle) intraperitoneally. Sham operated animals were operated similarly but without ligation of the LAD, and received injections with NaCl 0.9% w/v. After two days and three weeks LV function and IS were assessed by cardiac MRI. Three weeks post reperfusion LV fibrous content and LV wall thickness were evaluated histologically. Local inflammatory response was investigated two days and three weeks after MI-R injury using immunohistochemistry. The systemic inflammatory response was analyzed using ELISA and FACS. For further details see the Online Appendix.

Statistical analysis

Values were expressed as mean±SEM. Comparisons of parameters between the sham, PC-mAb, and vehicle groups were made using 1-way analysis of variance (ANOVA) with Tukey's correction or 2-way ANOVA with repeated measures and Tukey's post-test in case of multiple time points. Comparisons between PC-mAb and vehicle were made using unpaired t-tests. A value of $p < 0.05$ was considered to represent a significant difference. All statistical procedures were performed using IBM SPSS 23.0.0 (SPSS Inc – IBM, Armonk, NY, USA) and GraphPad Prism 6.02 (GraphPad Software Inc, La Jolla, CA, USA).

Results

Animal characteristics

Body weight (BW), heart weight (HW), total plasma cholesterol (TC) and triglyceride

(TG) concentrations were not affected following PC-mAb treatment (Table 1). HW/BW ratio was decreased following PC-mAb treatment compared to vehicle (5.9 ± 0.1 vs. 6.9 ± 0.3 mg/g, $p=0.025$). This suggest a reduction in cardiac hypertrophy following PC-mAb treatment.

Table 1: Plasma lipid profiles and animal characteristics

	T (wk)	sham	MI-R PC-mAb	MI-R vehicle
N		13	14	15
TC (mmol/L)	0	17.5 ± 1.7	17.4 ± 1.0	16.8 ± 1.3
TG (mmol/L)	0	2.5 ± 0.2	3.0 ± 0.2	2.6 ± 0.2
BW (g)	0	20.7 ± 0.5	21.5 ± 0.3	21.1 ± 0.4
	3	19.6 ± 0.3	20.8 ± 0.3	20.2 ± 0.4
HW (mg)	3	144 ± 8	123 ± 2	140 ± 7
HW/BW ratio (mg/g)	3	7.3 ± 0.3	$5.9 \pm 0.1^{* **}$	6.9 ± 0.3

Table 1: Plasma lipid levels and animal characteristics: plasma total cholesterol (TC), triglycerides (TG), body weight (BW), heart weight (HW). Values are means \pm SEM. $^{*}P<0.05$, vs. vehicle, $^{**}P<0.01$ vs. sham.

PC-mAb concentrations

To confirm the observed effects are indeed the result of PC-mAb treatment, we measured circulating PC-mAb levels two days and three weeks after MI-R injury. PC-mAb was not detectable in the sham and vehicle group both two days and three weeks after MI-R injury. In the PC-mAb treated group PC-mAb levels were 45 ± 10 μ g/ml after two days and 40 ± 10 μ g/ml after three weeks.

Contrast-enhanced MRI assessed infarct size

First, we assessed baseline IS two days post MI-R injury using contrast-enhanced MRI. No difference was observed between PC-mAb treated animals compared to vehicle animals ($28.3 \pm 1.4\%$ vs. $30.6 \pm 2.1\%$; Figure 1A). Three weeks after MI-R injury IS was significantly reduced in PC-mAb treated animals compared to vehicle animals ($12.8 \pm 1.2\%$ vs. $18.3 \pm 1.1\%$, $p=0.002$). Absolute IS was not different two days after MI-R injury between PC-mAb and vehicle treated animals (16.2 ± 1.0 mg vs. 16.7 ± 1.3 mg; Figure 1B), but three weeks after MI-R injury absolute IS was significantly reduced in PC-mAb treated animals compared to vehicle animals (6.3 ± 0.6 mg vs. 8.6 ± 0.5 mg, $p=0.006$). Non-infarcted myocardium (Figure 1C) was not significantly different between PC-mAb and vehicle animals at both two days (40.8 ± 1.4 mg vs. 37.9 ± 2.5 mg) and three weeks (42.5 ± 1.4 mg vs. 38.8 ± 2.1 mg). Taken together, this indicates IS significantly decreased following PC-mAb treatment when compared to vehicle animals three weeks after MI-R injury.

As expected some amount of infarct healing was observed in both groups, since IS was significantly smaller three weeks after MI-R injury when compared to two days after MI-R injury ($p<0.001$) as a result of transitory early infarct edema.

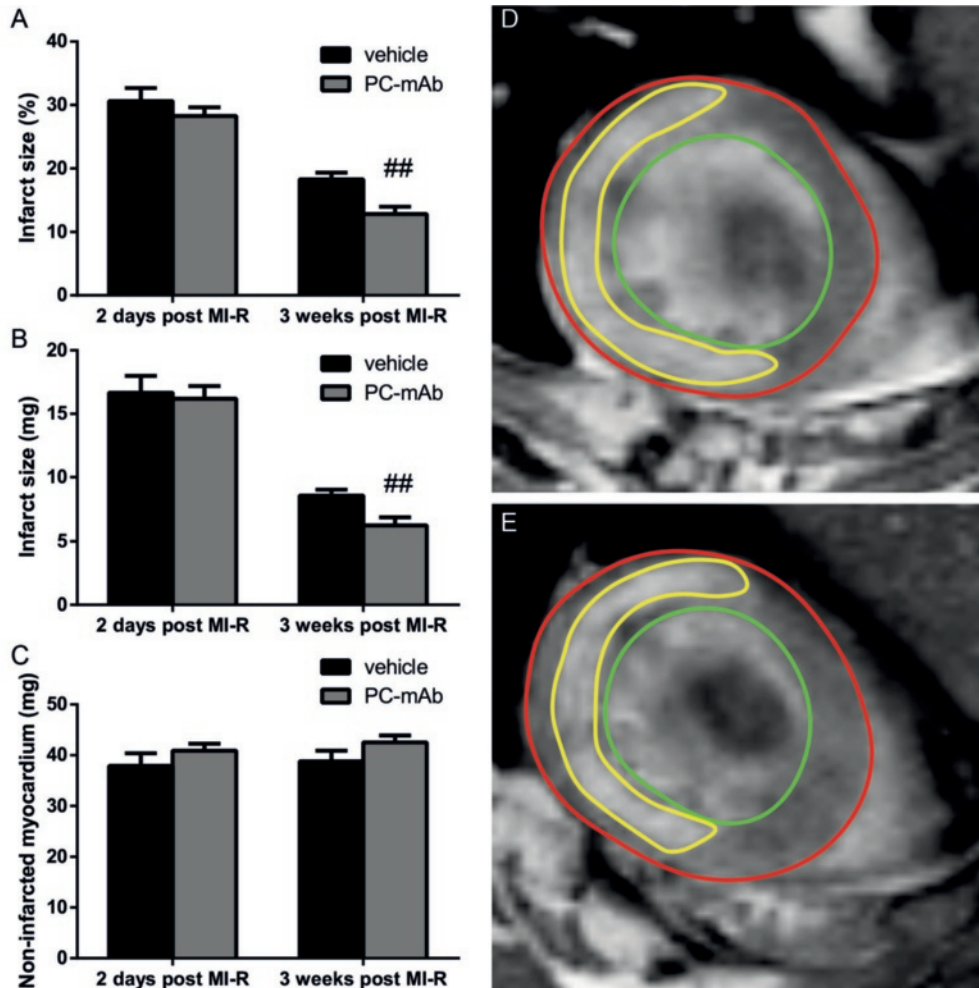


Figure 1: Quantification of infarct size using contrast-enhanced MR imaging. Infarct size was measured at baseline (two days post MI-R) and at sacrifice (three weeks post MI-R), infarct size is quantified as percentage of the LV mass (A), or as absolute mass (mg) of the infarcted myocardium (B; n=14-15 per group). (C) Absolute mass of the non-infarcted myocardium (mg). Representative Gd-DPTA-enhanced MR images two days post MI-R injury of vehicle (D) and PC-mAb treated (E) mice. Red line indicates epicardial border, green line indicates endocardial border and yellow line indicates infarct area. Data are mean±SEM. ^{##}p<0.01 vs. vehicle. LV dilation and function

To investigate the effect of PC-mAb treatment on LV dilatation and function, we made serial cine MRI images two days and three weeks post MI-R injury. Two days after MI-R injury EDV (Figure 2A) was not affected following PC-mAb treatment ($30.8 \pm 0.9 \mu\text{l}$) when compared to sham ($28.7 \pm 1.2 \mu\text{l}$) and vehicle ($34.4 \pm 2.3 \mu\text{l}$). However, three weeks after MI-R injury PC-mAb treatment resulted in significantly smaller EDV compared to vehicle animals ($33.7 \pm 1.4 \mu\text{l}$ vs. $44.4 \pm 2.4 \mu\text{l}$, $p < 0.001$), which was statistically not

different from the EDV of sham animals ($30.4 \pm 1.2 \mu\text{l}$). ESV (Figure 2B) was significantly increased two days after MI-R injury in both the vehicle ($19.4 \pm 2.0 \mu\text{l}$, $p < 0.001$) and PC-mAb group ($14.7 \pm 0.7 \mu\text{l}$, $p = 0.047$) compared to the sham group ($9.4 \pm 0.8 \mu\text{l}$), while no difference could be observed between the vehicle and PC-mAb group. Interestingly, three weeks post MI-R injury ESV was significantly smaller following PC-mAb treatment ($15.5 \pm 0.9 \mu\text{l}$) compared to vehicle animals ($26.6 \pm 2.2 \mu\text{l}$, $p < 0.001$), while no difference was observed when compared to the sham group ($11.2 \pm 1.0 \mu\text{l}$). Taken together, these results suggest PC-mAb treatment prevents LV dilatation to a level comparable to animals without MI-R injury.

EF as a measure of LV function (Figure 2C) was significantly decreased two days post MI-R injury in both the vehicle ($44.7 \pm 3.0\%$, $p < 0.001$) and PC-mAb group ($52.1 \pm 1.8\%$, $p < 0.001$) when compared to the sham group ($67.6 \pm 2.1\%$), while no difference was observed between vehicle and PC-mAb group. Three weeks post MI-R injury EF was still decreased in both vehicle ($40.8 \pm 2.9\%$, $p < 0.001$) and PC-mAb group ($54.1 \pm 1.8\%$, $p = 0.02$) when compared to sham ($63.9 \pm 2.3\%$). However, PC-mAb treatment significantly increased EF compared to vehicle animals ($p < 0.001$), indicating preservation of LV function by PC-mAb treatment, whereas EF further decreased in the vehicle group compared to the day two time point.

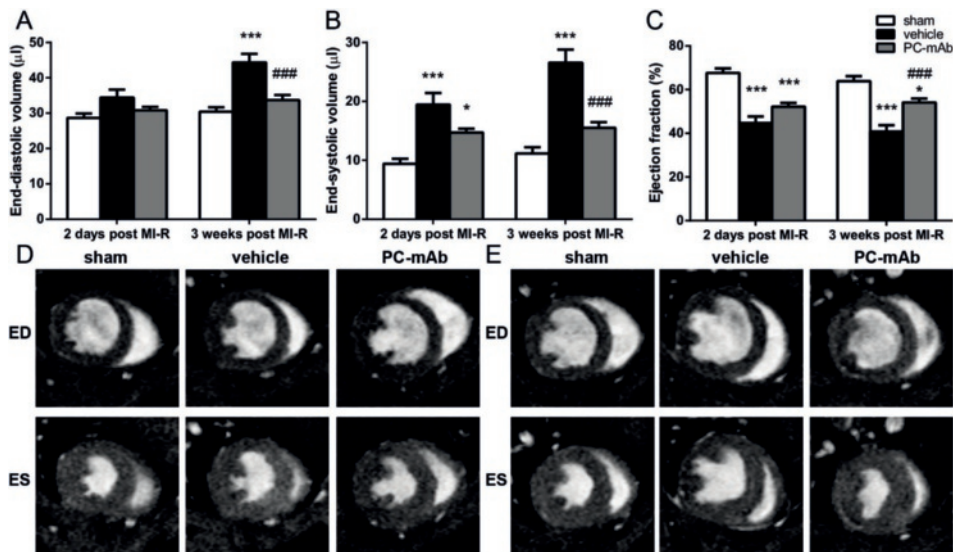


Figure 2: Quantification of LV volumes and function using cardiac MR imaging. LV volumes, EDV (A) and ESV (B), and function, EF (C), were assessed two days and three weeks after MI-R ($n=12-15$ per group). Representative transversal short-axis MR images at end-diastole (ED) and end-systole (ES) two days (D) and three weeks (E) post MI-R in the sham, vehicle and PC-mAb groups. Data are mean \pm SEM. ### $p < 0.05$ vs. vehicle, * $p < 0.05$, *** $p < 0.001$ both vs. sham.

LV fibrous content and LV wall thickness

To confirm the effect of PC-mAb on contrast-enhanced MRI assessed IS, we measured LV fibrous content, as a measure for IS, using Sirius Red staining. LV fibrous content was significantly reduced following PC-mAb treatment ($12.9 \pm 1.0\%$) compared to vehicle animals ($19.8 \pm 1.8\%$, $p=0.004$; Figure 3A), confirming the earlier observed decreased IS. Accordingly, three weeks after MI-R, LV wall thickness in the PC-mAb compared to the vehicle group was increased in the infarct area (0.87 ± 0.03 mm vs. 0.75 ± 0.04 mm, $p=0.045$) and border zones (1.13 ± 0.02 mm vs. 1.03 ± 0.03 mm, $p=0.041$). LV wall thickness in the interventricular septum was significantly increased in both the PC-mAb (1.18 ± 0.04 mm) and vehicle group (1.10 ± 0.04 mm) compared to the sham group (0.85 ± 0.04 mm, both $p<0.001$). These results indicate cardiac hypertrophy, probably caused by compensation of healthy cardiomyocytes to maintain cardiac function.

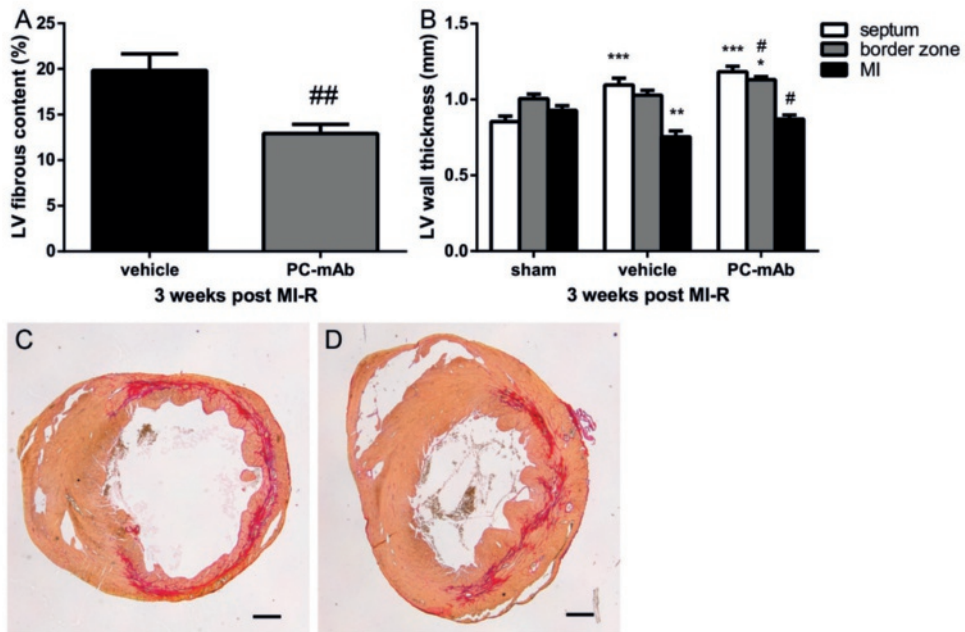


Figure 3: Histological quantification of LV fibrous content and LV wall thickness three weeks post MI-R. LV fibrous content (A) was measured by Sirius red staining and quantified as the area of the LV occupied by collagen. LV wall thickness (B) was assessed in 3 specific areas: interventricular septum, border zone and infarct area (n=9-10 per group). Representative images of Sirius Red staining of vehicle (C) and PC-Mab treated (D) mice. Scale bar = 500 μ m. Data are mean \pm SEM. # $p<0.05$, ## $p<0.01$ both vs. vehicle, * $p<0.05$, ** $p<0.01$, *** $p<0.001$ all vs. sham.

Local inflammatory response

To unravel the mechanism of PC-mAb treatment against MI-R injury, we investigated leukocyte infiltration two days and three weeks after MI-R injury using immunohistochemistry. First, we studied the early leukocyte infiltration two days post

MI-R injury in different areas of the LV wall namely: the interventricular septum, the border zones and in the infarct area (Figure 4A). In the interventricular septum (sham: 4.8 ± 0.7 , vehicle: 3.3 ± 1.1 and PC-mAb: 2.7 ± 0.6 leukocytes per 0.25 mm^2) no differences were observed between all groups. However, in the border zones we observed a near significant ($p=0.08$) reduction of leukocyte infiltration following PC-mAb treatment (4.2 ± 0.6 leukocytes per 0.25 mm^2) compared to vehicle animals (7.7 ± 2.2 leukocytes per 0.25 mm^2), but not compared to corresponding areas of the normal myocardium in sham animals (4.8 ± 0.4 leukocytes per 0.25 mm^2). In the infarct area we observed no significant difference between PC-mAb and vehicle treated mice (PC-mAb: 9.5 ± 1.5 vs. vehicle: 15.8 ± 4.7 leukocytes per 0.25 mm^2), but we did observe a significant increase in leukocyte infiltration in vehicle treated mice compared to sham (4.9 ± 0.4 leukocytes per 0.25 mm^2 , $p=0.01$).

Next, we investigated the leukocyte infiltration three weeks post MI-R injury in the same areas as mentioned before (Figure 4B). We observed a significant reduction of leukocyte infiltration in all areas following PC-mAb treatment compared to vehicle animals (septum: 0.8 ± 0.1 vs. 3.2 ± 0.7 , $p=0.001$, border zones: 1.1 ± 0.3 vs. 3.1 ± 0.4 , $p<0.001$, infarct area: 0.8 ± 0.2 vs. 3.4 ± 0.7 , $p<0.001$, leukocytes per 0.25 mm^2), while no difference was observed between the PC-mAb and sham group (septum: 1.2 ± 0.3 , border zones: 1.0 ± 0.2 , infarct area: 0.8 ± 0.1 leukocytes per 0.25 mm^2). Taken together, these results indicate that PC-mAb treatment reduces leukocyte infiltration.

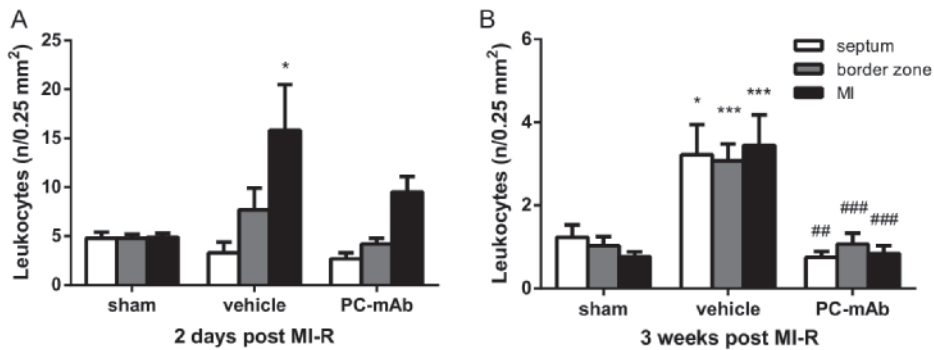


Figure 4: Histological quantification of the local inflammatory response. The number of CD45 positive cells (leukocytes) were counted per specific area: interventricular septum, border zone and infarct area, as measure of local inflammation. Each bar represents the average number of leukocytes per field of view in the specific areas 2 days post MI-R (A; $n=3-5$ per group) and three weeks post MI-R (B; $n=9-10$ per group). Data are mean \pm SEM. ## $p<0.01$, ### $p<0.001$ both vs. vehicle, * $p<0.01$, *** $p<0.001$ both vs. sham.

Systemic inflammatory response

To investigate the effect of PC-mAb treatment on the systemic inflammatory response after MI-R injury, we analyzed serum chemokine (C-C motif) ligand 2 (CCL2) levels two

days and three weeks post MI-R injury. Two days after MI-R injury PC-mAb treatment significantly reduces CCL2 levels compared to both vehicle and sham animals (PC-mAb: 13.4 ± 10.0 pg/ml, vehicle: 74.3 ± 6.6 pg/ml, $p=0.007$, sham: 80.5 ± 14.5 pg/ml, $p=0.002$; Figure 5A). Three weeks after MI-R injury the effect of PC-mAb treatment on CCL2 levels was less obvious. CCL2 levels were decreased, although not significantly, following

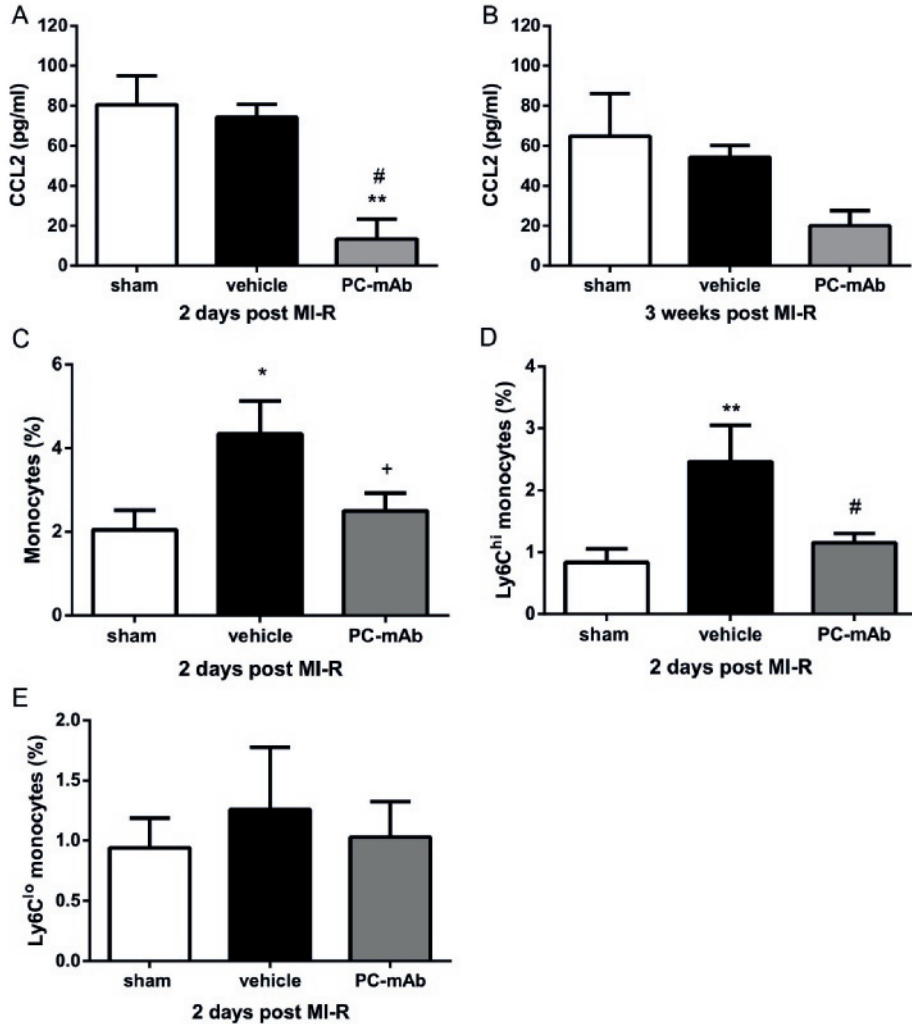


Figure 5: Quantification of the systemic inflammatory response. Serum levels of CCL2 were determined using ELISA as measure of systemic inflammation, two days post MI-R (A; $n=4-8$ per group) and three weeks post MI-R (B; $n=9-10$ per group). Circulating monocytes (C) and different monocyte subsets, Ly6C^{hi} (D) Ly6C^{lo} (E), were determined two days post MI-R using FACS analysis and expressed as percentage of total leukocytes ($n=4-8$ per group). Data are mean \pm SEM. + $p=0.09$, # $p<0.05$ both vs. vehicle, ** $p<0.01$ vs. sham.

PC-mAb treatment (20.0 ± 7.5 pg/ml; Figure 5B) compared to vehicle (54.2 ± 6.0 pg/ml) and sham animals (64.9 ± 21.3 pg/ml). Finally, we investigated the effect of PC-mAb treatment on circulating monocytes two days after MI-R injury. The percentage circulating monocytes (of total leukocytes) was near significantly ($p=0.09$) reduced following PC-mAb treatment ($2.5 \pm 0.4\%$) compared to vehicle animals ($4.3 \pm 0.8\%$), but not compared to sham animals ($2.0 \pm 0.5\%$; Figure 5C). Furthermore, the percentage circulating pro-inflammatory Ly6C^{hi} monocytes (of total leukocytes) was significantly reduced in the PC-mAb treated group ($1.2 \pm 0.2\%$) compared to the vehicle group ($2.5 \pm 0.6\%$, $p=0.02$), while no significant difference was observed when compared to the sham group ($0.8 \pm 0.2\%$; Figure 5D). Regarding the Ly6C^{lo} monocytes (Figure 5E) no significant differences were observed between all groups (sham: $0.9 \pm 0.2\%$; vehicle: $1.3 \pm 0.5\%$; PC-mAb: $1.0 \pm 0.3\%$ (percentage of total leukocytes)). Taken together, these results suggest that PC-mAb treatment especially reduces the early inflammatory response following MI-R injury.

Discussion

This study shows a therapeutic effect of PC-mAb treatment after MI-R injury. Administration of PC-mAb after MI-R injury attenuated the early systemic inflammatory response, by reduction of serum CCL2 levels and circulating Ly6C^{hi} monocytes after two days, as well as the late local inflammatory response by decreased myocardial leukocyte infiltration after three weeks. This resulted in a decreased IS and preservation of LV wall thickness which eventually caused restricted LV dilation and preserved LV function.

Post-ischemic LV remodeling and function

Adverse cardiac remodeling after a MI is characterized by an increase of both EDV and ESV, normally followed by a reduced EF²⁹. In this study we assessed EDV, ESV and EF and found PC-mAb treatment to significantly restrict EDV and ESV increase following MI-R injury accompanied by a significant increase in EF, thereby suggesting limitation of adverse cardiac remodeling with preservation of LV function.

We investigated the effect of PC-mAb treatment on IS using contrast-enhanced MRI and showed PC-mAb treatment to significantly decrease IS three weeks after MI-R injury. Previous research showed that IS is directly related to LV remodeling and clinical outcome following MI³⁰⁻³². This suggests the observed preservation of LV function to be the result of improved infarct healing as demonstrated by the reduced IS. In addition, we histologically supported this observation demonstrating a decreased LV fibrous content as a measure of IS and increased LV wall thickness following PC-mAb treatment. LV wall thickness is affected following a MI because of the loss of viable cardiomyocytes which are replaced by collagen³³. The preservation of LV wall thickness might indicate that

PC-mAb treatment restricts loss of viable cardiomyocytes. Furthermore, we observed an increase in LV wall thickness in the interventricular septum in both the PC-mAb and vehicle group, most likely the result of cardiac hypertrophy caused by compensation of healthy cardiomyocytes to maintain cardiac function³⁴.

Post-ischemic inflammatory response

Inflammation plays an important role in the repair process following MI leading to formation of a scar³⁵. Reperfusion itself causes additional damage to the myocardium by the formation of ROS⁴ and accelerates cell membrane damage of cardiomyocytes³⁶ making ischemic-reperfused myocardium amenable to anti-inflammatory interventions. We assessed the effect of PC-mAb treatment on the post-reperfusion inflammatory response by quantification of local infiltration of leukocytes in the LV wall, which was significantly decreased following PC-mAb treatment after three weeks. Infarct healing following MI-R injury can be divided into two phases, first the early inflammatory phase in which leukocytes play an important role by removing dead cells and matrix debris before they trigger the innate immune system, followed by a reparative phase in which the scar is formed³⁵. Our results suggest PC-mAb treatment to reduce the adverse long term inflammatory response, while the beneficial early inflammatory response is less affected as demonstrated by a non-significant difference in early leukocyte infiltration after two days.

CCL2 is an important chemokine responsible for the recruitment of leukocytes to injured tissue³⁷. Even though leukocytes remove possible immunogenic cell components and promote infarct healing after MI, CCL2 knock-out mice experience reduced macrophage recruitment to the infarcted myocardium, which resulted in decreased adverse ventricular remodeling following MI-R injury³⁸. In agreement with the above-mentioned study, we found that PC-mAb treatment resulted in significant reduction of CCL2 serum levels two days after MI-R injury. Previously, we demonstrated PC-mAb to reduce CCL2 production of monocytes stimulated with oxLDL *in vitro* and expression of CCL2 in cuffed femoral arteries *in vivo*²⁷. Systemic CCL2 levels are increased in ApoE*3-Leiden mice when fed a high fat diet³⁹. We suppose PC-mAb is capable of binding to apoptotic cells and/or oxLDL thereby reducing the systemic inflammatory response, as observed by reduced CCL2 levels, which subsequently may contribute to the reduction in adverse ventricular remodeling and preservation of cardiac function.

In addition, we observed a decrease of the percentage of monocytes in blood following PC-mAb treatment two days after reperfusion. As mentioned before, infarct healing can be divided in two different phases and in both phases a different subset of monocytes play their own specific role³⁵. In the inflammatory phase, pro-inflammatory Ly6C^{hi} monocytes, which can differentiate into pro-inflammatory M1 macrophages, contribute by clearing the infarct site from necrotic cells and matrix debris³⁵. In the reparative phase, anti-inflammatory Ly6C^{lo} monocytes, which can differentiate into repair associated

M2 macrophages, play an important role in scar formation and infarct healing³⁵. In this study we observed a decrease in Ly6C^{hi} monocytes, but not in Ly6C^{lo} monocytes. Thus, despite Ly6C^{hi} monocytes play an important role in clearing the infarct site from cell debris, we found a beneficial effect on infarct healing and LV function following a PC-mAb induced reduction of circulating Ly6C^{hi} monocytes. In agreement, it has been shown that hypercholesterolemia results in increased numbers of Ly6C^{hi} monocytes⁴⁰, subsequently leading to reduced EF⁴¹ and impaired infarct healing⁴².

Upon a myocardial ischemic event, affected cardiomyocytes can undergo apoptosis⁴³, thereby expressing oxidized molecules, like PC, on their outer membrane⁴⁴, which is immunogenic⁸. Previous research showed that natural and monoclonal EO6/T15 antibodies against PC are capable to bind to apoptotic cells and oxLDL^{12,13,44} thereby dampening the inflammatory response⁸. Therefore, we postulate that our PC-mAb antibodies reduce the inflammatory response following MI-R injury by binding to apoptotic cells before they trigger the innate immune system, subsequently leading to reduced adverse cardiac remodeling leading to preservation of cardiac function.

We performed this study in a clinically relevant setting by starting treatment after reperfusion and by using hypercholesterolemic mice. Most studies performed on possible therapeutic agents against MI-R injury used a strategy in which treatment was started before reperfusion was realized. In our opinion that is not really mimicking the clinical treatment of revascularized patients. Furthermore, hypercholesterolemia affects MI-R injury in mice⁴⁵⁻⁴⁷ and it is an important risk factor for MI in human⁴⁸. Vice versa, MI has been shown to accelerate atherosclerosis⁴⁹ indicating important interactions between both inflammatory processes. This makes them both amenable to anti-inflammatory and immunomodulatory treatment⁵⁰. We used ApoE*3-Leiden mice in this study, which develop hypercholesterolemia when fed a high cholesterol diet, but not when fed a chow diet⁵¹, mimicking the situation often observed in MI patients. The fact that we used a clinical relevant mouse model adds even more value to the already impressive cardioprotective effects of PC-mAb.

Conclusions

PC-mAb treatment attenuates the post-ischemic inflammatory response following myocardial ischemia reperfusion as demonstrated by a reduction of systemic CCL2 levels and circulating Ly6C^{hi} monocytes resulting in impaired myocardial leukocyte infiltration and preservation of LV wall thickness. In a translational animal model mimicking the clinical setting this resulted in limited adverse cardiac remodeling with a decreased infarct size causing reduced LV end-diastolic and end-systolic volumes accompanied by a preserved LV function. Therefore, PC-mAb therapy may be a valid therapeutic approach against MI-R injury.

References

- 1 McAloon, C. J. et al. The changing face of cardiovascular disease 2000-2012: An analysis of the world health organisation global health estimates data. *International journal of cardiology* 224, 256-264, doi:10.1016/j.ijcard.2016.09.026 (2016).
- 2 Bagai, A., Dangas, G. D., Stone, G. W. & Granger, C. B. Reperfusion strategies in acute coronary syndromes. *Circulation research* 114, 1918-1928, doi:10.1161/circresaha.114.302744 (2014).
- 3 Ibanez, B., Heusch, G., Ovize, M. & Van de Werf, F. Evolving therapies for myocardial ischemia/reperfusion injury. *Journal of the American College of Cardiology* 65, 1454-1471, doi:10.1016/j.jacc.2015.02.032 (2015).
- 4 Bagheri, F. et al. Reactive oxygen species-mediated cardiac-reperfusion injury: Mechanisms and therapies. *Life sciences*, doi:10.1016/j.lfs.2016.09.013 (2016).
- 5 Miller, Y. I. et al. Oxidation-specific epitopes are danger-associated molecular patterns recognized by pattern recognition receptors of innate immunity. *Circulation research* 108, 235-248, doi:10.1161/circresaha.110.223875 (2011).
- 6 Timmers, L. et al. Toll-like receptor 4 mediates maladaptive left ventricular remodeling and impairs cardiac function after myocardial infarction. *Circulation research* 102, 257-264, doi:10.1161/circresaha.107.158220 (2008).
- 7 Arslan, F. et al. Lack of fibronectin-EDA promotes survival and prevents adverse remodeling and heart function deterioration after myocardial infarction. *Circulation research* 108, 582-592, doi:10.1161/circresaha.110.224428 (2011).
- 8 Chang, M. K. et al. Apoptotic cells with oxidation-specific epitopes are immunogenic and proinflammatory. *The Journal of experimental medicine* 200, 1359-1370, doi:10.1084/jem.20031763 (2004).
- 9 Tsimikas, S. et al. Oxidation-specific biomarkers, lipoprotein(a), and risk of fatal and nonfatal coronary events. *Journal of the American College of Cardiology* 56, 946-955, doi:10.1016/j.jacc.2010.04.048 (2010).
- 10 Shaw, P. X. et al. Natural antibodies with the T15 idiotype may act in atherosclerosis, apoptotic clearance, and protective immunity. *The Journal of clinical investigation* 105, 1731-1740, doi:10.1172/jci8472 (2000).
- 11 Palinski, W. et al. Cloning of monoclonal autoantibodies to epitopes of oxidized lipoproteins from apolipoprotein E-deficient mice. Demonstration of epitopes of oxidized low density lipoprotein in human plasma. *The Journal of clinical investigation* 98, 800-814, doi:10.1172/jci118853 (1996).
- 12 Horkko, S. et al. Monoclonal autoantibodies specific for oxidized phospholipids or oxidized phospholipid-protein adducts inhibit macrophage uptake of oxidized low-density lipoproteins. *The Journal of clinical investigation* 103, 117-128, doi:10.1172/jci4533 (1999).
- 13 Chang, M. K. et al. Monoclonal antibodies against oxidized low-density lipoprotein bind to apoptotic cells and inhibit their phagocytosis by elicited macrophages: evidence that oxidation-specific epitopes mediate macrophage recognition. *Proceedings of the National Academy of Sciences of the United States of America* 96, 6353-6358 (1999).
- 14 Huber, J. et al. Oxidized membrane vesicles and blebs from apoptotic cells contain biologically active oxidized phospholipids that induce monocyte-endothelial interactions. *Arteriosclerosis, thrombosis, and vascular biology* 22, 101-107 (2002).
- 15 Kyaw, T. et al. B1a B lymphocytes are atheroprotective by secreting natural IgM that increases IgM deposits and reduces necrotic cores in atherosclerotic lesions. *Circulation research* 109, 830-840, doi:10.1161/circresaha.111.248542 (2011).
- 16 Rosenfeld, S. M. et al. B-1b Cells Secrete Atheroprotective IgM and Attenuate Atherosclerosis. *Circulation research* 117, e28-39, doi:10.1161/circresaha.117.306044 (2015).
- 17 Tsiantoulas, D., Gruber, S. & Binder, C. J. B-1 cell immunoglobulin directed against oxidation-specific epitopes. *Frontiers in immunology* 3, 415, doi:10.3389/fimmu.2012.00415 (2012).
- 18 Grasset, E. K. et al. Sterile inflammation in the spleen during atherosclerosis provides oxidation-specific epitopes that induce a protective B-cell response. *Proceedings of the National Academy of Sciences of the United States of America* 112, E2030-2038, doi:10.1073/pnas.1421227112 (2015).
- 19 de Faire, U. et al. Low levels of IgM antibodies to phosphorylcholine predict cardiovascular disease in 60-year old men: effects on uptake of oxidized LDL in macrophages as a potential mechanism. *Journal of autoimmunity* 34, 73-79, doi:10.1016/j.jaut.2009.05.003 (2010).
- 20 Gleissner, C. A. et al. Low levels of natural IgM antibodies against phosphorylcholine are independently associated with vascular remodeling in patients with coronary artery disease. *Clinical research in cardiology : official journal of the German Cardiac Society* 104, 13-22, doi:10.1007/s00392-014-0750-y (2015).
- 21 Gronlund, H. et al. Low levels of IgM antibodies against phosphorylcholine predict development of acute myocardial infarction in a population-based cohort from northern Sweden. *European journal of cardiovascular prevention and rehabilitation : official journal of the European Society of Cardiology, Working Groups on Epidemiology & Prevention and Cardiac Rehabilitation and Exercise Physiology* 16, 382-386, doi:10.1097/HJR.0b013e32832a05df (2009).
- 22 Gigante, B. et al. Low levels of IgM antibodies against phosphorylcholine are associated with fast carotid intima media thickness progression and cardiovascular risk in men. *Atherosclerosis* 236, 394-399, doi:10.1016/j.

atherosclerosis.2014.07.030 (2014).

- 23 Caidahl, K. et al. IgM-phosphorylcholine autoantibodies and outcome in acute coronary syndromes. *International journal of cardiology* 167, 464-469, doi:10.1016/j.ijcard.2012.01.018 (2013).
- 24 Caligiuri, G. et al. Phosphorylcholine-targeting immunization reduces atherosclerosis. *Journal of the American College of Cardiology* 50, 540-546, doi:10.1016/j.jacc.2006.11.054 (2007).
- 25 Binder, C. J. et al. Pneumococcal vaccination decreases atherosclerotic lesion formation: molecular mimicry between *Streptococcus pneumoniae* and oxidized LDL. *Nature medicine* 9, 736-743, doi:10.1038/nm876 (2003).
- 26 Faria-Neto, J. R. et al. Passive immunization with monoclonal IgM antibodies against phosphorylcholine reduces accelerated vein graft atherosclerosis in apolipoprotein E-null mice. *Atherosclerosis* 189, 83-90, doi:10.1016/j.atherosclerosis.2005.11.033 (2006).
- 27 Ewing, M. M. et al. Optimized anti-phosphorylcholine IgG for therapeutic inhibition of inflammatory vascular disease. *European heart journal* 34, P5703-P5703, doi:10.1093/eurheartj/ehs310.P5703 (2013).
- 28 Michael, L. H. et al. Myocardial infarction and remodeling in mice: effect of reperfusion. *The American journal of physiology* 277, H660-668 (1999).
- 29 Galli, A. & Lombardi, F. Postinfarct Left Ventricular Remodelling: A Prevailing Cause of Heart Failure. *Cardiology research and practice* 2016, 2579832, doi:10.1155/2016/2579832 (2016).
- 30 Wu, E. et al. Infarct size by contrast enhanced cardiac magnetic resonance is a stronger predictor of outcomes than left ventricular ejection fraction or end-systolic volume index: prospective cohort study. *Heart (British Cardiac Society)* 94, 730-736, doi:10.1136/hrt.2007.122622 (2008).
- 31 Masci, P. G. et al. Relationship between location and size of myocardial infarction and their reciprocal influences on post-infarction left ventricular remodelling. *European heart journal* 32, 1640-1648, doi:10.1093/eurheartj/ehs064 (2011).
- 32 McAlindon, E., Bucciarelli-Ducci, C., Suleiman, M. S. & Baumbach, A. Infarct size reduction in acute myocardial infarction. *Heart (British Cardiac Society)* 101, 155-160, doi:10.1136/heartjnl-2013-304289 (2015).
- 33 Sutton, M. G. & Sharpe, N. Left ventricular remodeling after myocardial infarction: pathophysiology and therapy. *Circulation* 101, 2981-2988 (2000).
- 34 Shimizu, I. & Minamino, T. Physiological and pathological cardiac hypertrophy. *Journal of molecular and cellular cardiology* 97, 245-262, doi:10.1016/j.yjmcc.2016.06.001 (2016).
- 35 Prabhu, S. D. & Frangogiannis, N. G. The Biological Basis for Cardiac Repair After Myocardial Infarction: From Inflammation to Fibrosis. *Circulation research* 119, 91-112, doi:10.1161/circresaha.116.303577 (2016).
- 36 Hori, M. & Nishida, K. Oxidative stress and left ventricular remodelling after myocardial infarction. *Cardiovascular research* 81, 457-464, doi:10.1093/cvr/cvn335 (2009).
- 37 Gillitzer, R. & Goebeler, M. Chemokines in cutaneous wound healing. *Journal of leukocyte biology* 69, 513-521 (2001).
- 38 Dewald, O. et al. CCL2/Monocyte Chemoattractant Protein-1 regulates inflammatory responses critical to healing myocardial infarcts. *Circulation research* 96, 881-889, doi:10.1161/01.RES.0000163017.13772.3a (2005).
- 39 Murphy, N. et al. Dietary antioxidants decrease serum soluble adhesion molecule (sVCAM-1, sICAM-1) but not chemokine (JE/MCP-1, KC) concentrations, and reduce atherosclerosis in C57BL but not apoE*3 Leiden mice fed an atherogenic diet. *Disease markers* 21, 181-190 (2005).
- 40 Swirski, F. K. et al. Ly-6Chi monocytes dominate hypercholesterolemia-associated monocytoysis and give rise to macrophages in atheromata. *The Journal of clinical investigation* 117, 195-205, doi:10.1172/jci29950 (2007).
- 41 Panizzi, P. et al. Impaired infarct healing in atherosclerotic mice with Ly-6C(hi) monocytoysis. *Journal of the American College of Cardiology* 55, 1629-1638, doi:10.1016/j.jacc.2009.08.089 (2010).
- 42 Nahrendorf, M. et al. The healing myocardium sequentially mobilizes two monocyte subsets with divergent and complementary functions. *The Journal of experimental medicine* 204, 3037-3047, doi:10.1084/jem.20070885 (2007).
- 43 Frangogiannis, N. G. The immune system and cardiac repair. *Pharmacological research* 58, 88-111, doi:10.1016/j.phrs.2008.06.007 (2008).
- 44 Chou, M. Y. et al. Oxidation-specific epitopes are dominant targets of innate natural antibodies in mice and humans. *The Journal of clinical investigation* 119, 1335-1349, doi:10.1172/jci36800 (2009).
- 45 Girod, W. G., Jones, S. P., Sieber, N., Aw, T. Y. & Lefer, D. J. Effects of hypercholesterolemia on myocardial ischemia-reperfusion injury in LDL receptor-deficient mice. *Arteriosclerosis, thrombosis, and vascular biology* 19, 2776-2781 (1999).
- 46 Scalia, R. et al. Simvastatin exerts both anti-inflammatory and cardioprotective effects in apolipoprotein E-deficient mice. *Circulation* 103, 2598-2603 (2001).
- 47 Jones, S. P., Girod, W. G., Marotti, K. R., Aw, T. Y. & Lefer, D. J. Acute exposure to a high cholesterol diet attenuates myocardial ischemia-reperfusion injury in cholesteryl ester transfer protein mice. *Coronary artery disease* 12, 37-44 (2001).
- 48 Yusuf, S. et al. Effect of potentially modifiable risk factors associated with myocardial infarction in 52 countries (the INTERHEART study): case-control study. *Lancet (London, England)* 364, 937-952, doi:10.1016/s0140-6736(04)17018-

9 (2004).
49 Dutta, P. et al. Myocardial infarction accelerates atherosclerosis. *Nature* 487, 325-329, doi:10.1038/nature11260
(2012).
50 Frostegard, J. Immunity, atherosclerosis and cardiovascular disease. *BMC medicine* 11, 117, doi:10.1186/1741-
7015-11-117 (2013).
51 Lardenoye, J. H. et al. Accelerated atherosclerosis by placement of a perivascular cuff and a cholesterol-rich diet
in ApoE*3Leiden transgenic mice. *Circulation research* 87, 248-253 (2000).

Supplemental material

Methods

Animals and diets

All animal experiments were approved by the Institutional Committee for Animal Welfare of the Leiden University Medical Center (LUMC) and in compliance with Dutch government guidelines and the Directive 2010/63/EU of the European Parliament. Transgenic female ApoE*3-Leiden mice¹, backcrossed for more than 40 generations on a C57Bl/6J background (bred in the animal facility of the LUMC), aged 8-10 weeks at the start of a dietary run-in period were used for this experiment. Mice were fed a semisynthetic Western-type diet supplemented with 0.4% cholesterol (AB Diets, Woerden, The Netherlands) four weeks prior to surgery which was continued throughout the complete experiment. Mice were housed under standard conditions in conventional cages and received food and water ad libitum.

Plasma lipid analysis

Plasma levels of total cholesterol (TC) and triglycerides (TG) were determined for randomization one week before surgery. After a 4-hour fasting period, plasma was obtained via tail vein bleeding and assayed for total cholesterol (TC) and triglycerides (TG) levels using commercially available enzymatic kits according to the manufacturer's protocols (11489232; Roche Diagnostics, Mannheim, Germany, and 11488872; Roche Diagnostics, Mannheim, Germany, respectively).

Surgical myocardial infarction models and PC-mAb injections

Myocardial ischemia-reperfusion (MI-R) injury was induced at day 0 in 12-14 weeks old female ApoE*3-Leiden mice as described previously². Briefly, mice were pre-anesthetized with 5% isoflurane in a gas mixture of oxygen and room air and placed in a supine position on a heating pad. After endotracheal intubation and ventilation (rate 160 breaths/min, stroke volume 190 μ L; Harvard Apparatus, Holliston, MA, USA), mice were kept anesthetized with 1.5-2% isoflurane. Subsequently, a left thoracotomy was performed in the 4th intercostal space and the left anterior descending (LAD) coronary artery was ligated during 45 minutes using a 7-0 prolene suture knotted on a 2 mm section of a plastic tube. Ischemia was confirmed by myocardial blanching. After 45 minutes of ischemia, permanent reperfusion was established. Subsequently, the thorax was closed in layers with 5-0 prolene suture and mice were allowed to recover. Analgesia was obtained with buprenorphine s.c. (0.1 mg/kg) pre-operative and 10-12 hours post-operative. After surgery, animals were randomly grouped to receive intraperitoneal injections with 10 mg/kg PC-mAb every 3rd day or NaCl 0.9% w/v as a control (vehicle). Sham operated animals were operated similarly but without ligation of the LAD, and

received intraperitoneal injections with NaCl 0.9% w/v. Injections were administered direct after surgery (approximately 15 minutes after reperfusion) and between 12:00 p.m. and 2:00 p.m. every 3rd day thereafter.

After two days or three weeks mice were euthanized by bleeding and explantation of the heart under general anesthesia with 1.5-2% isoflurane and heart weight (HW) was determined using a digital scale. Next, hearts were immersion-fixed in 4% paraformaldehyde for 24 hours and embedded in paraffin. Blood samples were collected and used for serum analysis. The heart and body weights were measured from all animals.

Cardiac magnetic resonance imaging

Left ventricular (LV) dimensions and function were assessed two and three weeks after surgery by using a 7-Tesla magnetic resonance imaging (MRI) (Bruker Biospin, Ettlingen, Germany) to obtain contrast-enhanced and cine MRI images. Mice were pre-anesthetized with 5% isoflurane and maintained anesthetized at 1-2% isoflurane. Respiratory rate was monitored by a respiration detection cushion, which was placed underneath the thorax and connected to a gating module to monitor respiratory rate (SA Instruments, Inc., Stony Brook, NY). Image reconstruction was performed using Bruker ParaVision 5.1 software.

Infarct size

To distinguish for any possible treatment effect initial baseline IS was determined at day two using contrast-enhanced MR imaging after injection of a 150 μ L (0.05 mmol/ml) bolus of gadolinium-DPTA (Gd-DPTA, Dotarem, Guerbet, The Netherlands) via the tail vein. A high-resolution 2D FLASH cine sequence was used to acquire a set of 14 contiguous 0.5 mm slices in short-axis orientation covering the entire heart. Imaging parameters were: echo time of 1.9 ms, repetition time of 84.16 ms, field of view of 33 mm², and a matrix size of 192x256.

Mice without visible contrast were excluded from the study as being failed MI procedure. Therapeutic effects regarding IS were determined by repetition of contrast-enhanced MRI at day 21.

LV dimensions and function

LV dimensions were measured at day two and after three weeks with a high-resolution 2D fast gradient echo (FLASH) sequence to acquire a set of contiguous 1 mm slices in short-axis orientation covering the entire long-axis of the heart. Imaging parameters were: echo time of 1.49 ms, repetition time of 5.16 ms, field of view of 26 mm², and a matrix size of 144x192.

Image analysis

MRI images were converted to DICOM format and analyzed with the MR Analytical Software System (MASS) for mice (MEDIS, Leiden, The Netherlands). LV endo- and epicardial borders were delineated manually by an investigator blinded to the experimental groups. End-diastolic and end-systolic phases and the contrast enhanced areas were identified automatically, and the percentage of infarcted myocardium, LV end-diastolic volume (EDV), LV end-systolic volume (ESV), and LV ejection fraction (EF) were computed.

LV fibrous content and LV wall thickness

Paraffin-embedded hearts were cut into serial transverse sections of 5 μm along the entire long-axis of the LV. To analyze collagen deposition as an indicator of the fibrotic area, every 50th section of each heart was stained with Sirius Red. LV fibrous content was determined by planimetric measurement of all sections and calculated as fibrotic area divided by the total LV wall surface area including the interventricular septum.

LV wall thickness was measured in five different sections centralized in the infarct area. Per section, wall thickness was analyzed at 3 places equally distributed in the infarcted area, both border zones, and 2 places of the interventricular septum. Measurements were performed perpendicular to the ventricular wall. Corresponding areas were used for measurements in the non-infarcted sham group. All measurements were performed by an observer blinded to the groups, using the ImageJ 1.47v software program (NIH, USA).

Myocardial inflammatory response

For analysis of the cardiac inflammatory response a subpopulation was selected, and sections of the mid-infarct region of the heart were stained using antibodies against leukocytes (anti-CD45, 550539; BD Pharmingen, San Diego, CA, USA). The number of leukocytes was expressed as a number per 0.25 mm² in the septum (2 areas), border zones (2 areas), and infarcted myocardium (3 areas). Corresponding areas were used for measurements in the non-infarcted sham group.

FACS analysis

To examine the effect of PC-mAb therapy on the acute inflammatory response, mice were euthanized and blood samples were collected at day two. To study the systemic effects whole blood was analyzed for monocytosis. White blood cell counts (WBC, $\times 10^6/\text{mL}$) were measured using a semi-automatic hematology analyzer F-820 (Sysmex; Sysmex Corporation, Etten-Leur, The Netherlands). For FACS analysis, 35 μL of whole blood was incubated for 30 min on ice with directly conjugated antibodies directed against Ly6C-FITC (AbD Serotec, Dusseldorf, Germany), Ly6G-PE (BD Pharmingen, San Diego, CA, USA), CD11b-APC (BD Pharmingen, San Diego, CA, USA), and CD115-PerCP (R&D Systems, Minneapolis, MN, USA). Monocytes were gated based on their expression

profile: CD11b-positive, Ly6G-negative, and CD115-positive. Data was analyzed using FlowJo software (Tree Star Inc.)

CCL2 and PC-mAb ELISA

An PC-mAb ELISA kit (Athera Biotechnologies, Solna, Sweden) was used to determine serum PC-mAb concentrations. To study the effects of PC-mAb on systemic inflammation, an ELISA kit (Cat. No. 555260, BD Biosciences, San Diego, CA, USA) for cytokine concentration of chemokine (C-C motif) ligand 2 (CCL2) was used.

Statistical analysis

Values were expressed as mean \pm SEM. Comparisons of parameters between the sham, PC-mAb, and vehicle groups were made using 1-way analysis of variance (ANOVA) with Tukey's correction or 2-way ANOVA with repeated measures and Tukey's posttest in case of multiple time points. Comparisons between PC-mAb and vehicle were made using unpaired t-tests. A value of $p < 0.05$ was considered to represent a significant difference. All statistical procedures were performed using IBM SPSS 23.0.0 (SPSS Inc – IBM, Armonk, NY, USA) and GraphPad Prism 6.02 (GraphPad Software Inc, La Jolla, CA, USA).

References

- 1 van den Maagdenberg, A. M. et al. Transgenic mice carrying the apolipoprotein E3-Leiden gene exhibit hyperlipoproteinemia. *The Journal of biological chemistry* 268, 10540-10545 (1993).
- 2 Michael, L. H. et al. Myocardial infarction and remodeling in mice: effect of reperfusion. *The American journal of physiology* 277, H660-668 (1999).